JSES International 7 (2023) 104–112

Contents lists available at ScienceDirect

JSES International

journal homepage: www.jsesinternational.org

Proximal humerus fracture sequelae: are corrective osteotomies still a taboo? The role of three-dimensional preoperative planning and patient-specific surgical guides for proximal humerus corrective osteotomy in combination with reverse shoulder arthroplasty

Andrea Cozzolino, MD[a], Antonio Guastafierro, MD[b], Alessio Bernasconi, PhD[a], Giuseppe Della Rotonda, MD[b], Paolofrancesco Malfi, MD[a], Alfonso Fedele, MD[b], Marco Mortellaro, MSc[b], Paolo Minopoli, BSc[b], Livia Renata Pietroluongo, MSc[b], Raffaele Russo, MD[a,*]

[a]Department of Public Health, University of Naples Federico II, Naples, Italy
[b]Department of Orthopedic Surgery, Pineta Grande Hospital, Castelvolturno, Italy

ARTICLE INFO

Keywords:
Three-dimensional
Patient-specific instrumentation
Humerus
Malunion
Virtual planning
3D printing
Fractures sequelae
Shoulder arthroplasty

Level of evidence: Level IV; Case Series; Treatment Study

Background: Symptomatic proximal humeral fracture sequelae (PHFS) represent a surgical challenge due to the altered bone and soft tissue morphology. The purpose of this study was to report the outcome of Multiplanar Corrective Humeral Osteotomies (MCHOs) in combination with reverse total shoulder arthroplasty (rTSA) performed following a three-dimensional (3D) preoperative planning and using a 3D-printed patient-specific surgical instrumentation (PSI) in type 1C, 1D, and 4 PHFS.

Methods: In this prospective monocentric study, we enrolled patients affected by symptomatic PHFS type 1C, 1D, or 4 of Boileau's classification, treated between 2018 and 2019 with rTSA associated to MCHO and followed-up at 12 and 24 mo. The preoperative and postoperative Constant Score (CS), visual analog scale, and Disabilities of the Arm, Shoulder and Hand (DASH) score were recorded. All patients underwent a preoperative computed tomography, then a dedicated software was used to run a segmentation algorithm on computed tomography images. Metaphyseal bone cuts were virtually performed before surgery in all patients, and a 3D-printed PSI was used to reproduce the planned osteotomies in vivo.

Results: Twenty patients completed a 2-y follow-up. The mean (± standard deviation) CS, visual analog scale, and DASH values improve from 24.3 (± 8.8), 6.5 (± 1.3), 60.7 (± 9.6) preoperatively, to 67.7 (± 11.4), 1.6 (± 0.8), 24.1 (± 13.1) points after surgery, respectively. The minimally clinical important difference for CS and DASH score was achieved in 95% of patients. No major complication was observed. One patient showed an unexplained worsening of clinical scores between the 12 and the 24-mo follow-up, while in one patient bone resorption of the greater tuberosity was observed on radiographs at 2 y, with no clinical impact.

Conclusion: The combination of preoperative 3D planning and intraoperative use of 3D-printed PSI to perform MCHO as concurrent procedure in the context of rTSA in the treatment of Boileau type 1C, 1D, and 4 PHFS may lead to a satisfactory clinical outcome at 2 y of follow-up.

Proximal humeral fracture sequelae (PHFS) are a cause of shoulder stiffness, significant chronic pain, and disability.[1,2,11,18,19,24] In 2001, Boileau et al classified PHFS into 4 main types according to the level of the deformity (intracapsular or extracapsular) and to the status of the tuberosities.[7] In 2012, the same author updated the classification system by adding 4 different subgroups to type 1, that is, type 1A in presence of osteonecrosis, type 1B for post-traumatic arthritis, type 1C and 1D for valgus and varus malunion, respectively.[19]

In case of symptomatic PHFS, the surgical treatment may vary from corrective osteotomies to hemiarthroplasty, anatomic, or reverse total shoulder arthroplasty (rTSA).[5,17,24,27,31,37,40,46] It is known that the functional outcome after surgery in patients with malunion is generally less satisfactory than the one achieved in

Local ethical committee approval was obtained by the local health authority (Comitato Scientifico Campania Nord - A.S.L. Caserta). Study N°1269876/AAGG. Via G.Carducci 42, 80121. Naples, Italy.

*Corresponding author: Raffaele Russo, MD, Department of Orthopedic Surgery, Pineta Grande Hospital, Castelvolturno (CE), Italy.
E-mail address: raff.russo55@gmail.com (R. Russo).

https://doi.org/10.1016/j.jseint.2022.09.016

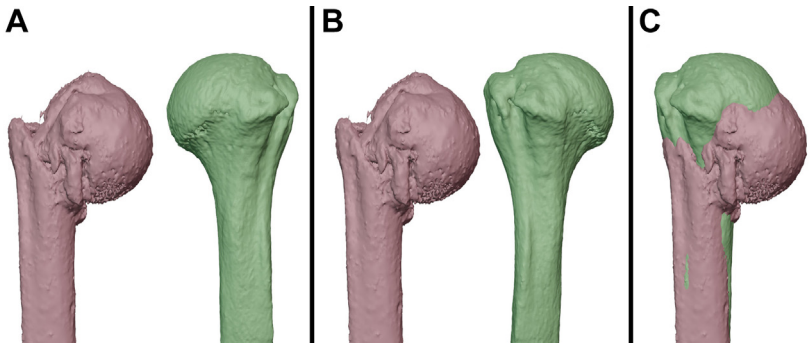

Figure 1 3D assessment of the malunion. 3D models of the pathologic humerus (*purple*) and the healthy contralateral humerus (*green*) were generated using a segmentation software (**A**). The healthy contralateral humerus (*green*) was mirrored (**B**) and superimposed to the pathological model (**C**) to appreciate and measure the deviations of the deformity. Reproduced by permission of Russo R, Cozzolino A, Guastafierro A, Della Rotonda G, Viglione S, Ciccarelli M, Mortellaro M, Minopoli P, Fiorentino F, Pietroluongo LR, and Wolters Kluwer Health, Inc. Use of 3D planning and patient-specific guide for proximal humerus corrective osteotomy associated with shoulder prosthesis implantation in proximal humerus varus malunion. Tech Hand Up Extrem Surg 2021. Further reproduction, distribution, or transmission is prohibited, except as otherwise permitted by law. *3D*, three-dimensional.

Table I
Differences between PHFS types according to greater tuberosity position and rotator cuff status.

PHFS type	1A – 1B - 2	1C	1D	4A
GT position	undisplaced 1C - 1D - 4A	lateral to diaphysis	medial to diaphysis 4B	medial to the humeral head
Posterior rotator cuff	Reparable if: infraspinatus and teres minor fat atrophy is graded as Goutallier ≤3 or ≤2, respectively		Irreparable if: infraspinatus and teres minor fat atrophy is graded as Goutallier > 3, or > 2, respectively	

GT, greater tuberosity; *PHFS*, proximal humeral fracture sequelae.

patients treated acutely, with an associated higher risk of complication.[4,8,10,18] This may be explained by the longer delay between trauma and surgery, the amount of tuberosity displacement, the chronic soft tissue retraction, the metaphyseal bone loss, the complexity of revision surgery after failed osteosynthesis, and the patient functional expectations.[6,11,13,23,35]

In particular, PHFS types 1C, 1D, and 4 represent a surgical challenge due to the high anatomical variability of the proximal humerus, the difficulties encountered during the positioning of the humeral prosthetic stem[7] and the absence of a standardized approach to these patients. Interestingly, many authors have advised against performing greater tuberosity osteotomies in the setting of prosthetic replacement of the shoulder due to the poor clinical outcome and the high complication rate.[6] On the other side, during the last years, three-dimensional (3D) virtual preoperative planning and custom-made surgical guides have been made available and proven as valuable aids in this kind of surgery,[12,29,42] enabling surgeons to evaluate post-traumatic deformities in a 3D environment and to plan osteotomies with greater accuracy.[43,44]

With this background, we performed a study aimed 1) to identify PHFS subgroups requiring similar osteotomy patterns and 2) to report the outcome of Multiplanar Corrective Humeral Osteotomies (MCHOs) performed following a 3D preoperative planning and using a 3D-printed patient-specific surgical instrumentation (PSI) in type 1C, 1D, and 4 PHFS as concurrent procedures in rTSA.

Methods

Study design

After Local Ethical Committee approval, a prospective monocentric study was conducted at the 'Second Orthopaedic Unit' of the 'Pineta Grande Hospital' (Castel Volturno, Italy) from January 2018 to December 2019, enrolling patients presenting with type 1C, 1D, and 4 symptomatic PHFS treated with MCHO in combination to rTSA. Exclusion criteria were isolated post-traumatic arthritis or humeral head necrosis (PHFS types 1A and 1B), PHFS associated to chronic glenohumeral dislocation (PHFS type 2), PHFS in which a MCHO was not part of the surgical strategy, patients treated with an isolated MCHOs, and patients affected by infection.

Algorithm of treatment

A stepwise approach was systematically applied to all patients, including: 1) a preoperative 3D assessment of the deformity, 2) planning and virtual reproduction of the MCHO, 3) design of PSI (cutting guides), and 4) surgery.

Preoperative 3D assessment of the deformity

A 64-slice computed tomography (CT) scan of the shoulder was performed in all cases. Digital Imaging and COmmunications in Medicine images were then elaborated using a dedicated software for segmentation (Mimics 22, Materialize, Leuven, Belgium) (Fig. 1*A*) in order to generate a 3D model of the humerus. The deformity was quantified based on a comparison with either the healthy contralateral side (if available) or the standard values reported in literature.[9,12,16] The healthy contralateral model was mirrored and superimposed onto the pathologic model (Fig 1*A-C*) (overlap method) which allowed to measure the degree of displacement and rotation of bony parts.

Ten anatomic variables were recorded for each case as shown in Tables I and II.

According to the aforementioned 10 variables, 4 different anatomic scenarios were identified, which led us to introduce a new subtype (4B) to the Boileau and Moineau classification, as follows:

- Type 1C – Valgus displaced malunion with the greater tuberosity positioned lateral to the diaphysis; usually associated to

Table II
Preoperative demographic and radiological data of included patients according to the type of PHFS.

	Type 1C	Type 1D	Type 4A	Type 4B	Total
No. of patients	4	8	6	2	20
Age mean ± SD (y)	71.7 ± 6.8	74.5 ± 4.4	69 ± 4.5	49 ± 3	69.7 ± 8.8
Gender (M/F)	0/4	1/7	0/6	1/1	2/18
Previous treatment (conservative/surgical)	4/0	5/3	4/2	0/2	13/7
Delta time mean ± SD (mo)	9.6 ± 3.3	8 ± 7.4	52.3 ± 68.2	10 ± 2	25.2 ± 47
Neck shaft angle mean ± SD (°)	165 ± 12	100 ± 19	159 ± 35	210 ± 10	141 ± 44
Torsion angle mean ± SD (°)	−30 ± 15	−33 ± 24	−23 ± 16	−135 ± 15	−47 ± 48
Anteroposterior tilt mean ± SD (°)	−25 ± 10	−8 ± 23	−14 ± 14	−22 ± 12	−12 ± 18
Coronal translation mean ± SD (mm)	−15 ± 7	6 ± 10	1 ± 4	2 ± 2	0 ± 11
Parasagittal translation mean ± SD (mm)	1.5 ± 3.5	−6 ± 9.1	0.8 ± 1.8	4 ± 4	−1.6 ± 7.4
Arthritis	2	2	3	2	9
Humeral Head Necrosis	2	1	1	0	4

PHFS, proximal humeral fracture sequelae; *SD*, standard deviation.

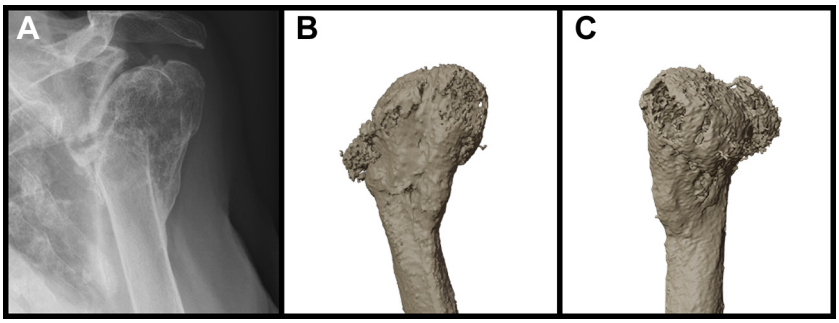

Figure 2 Type 1C PHFS. (**A**) true anteroposterior radiograph view, (**B**) coronal 3D CT scan, and (**C**) sagittal 3D CT scan view of a valgus displaced proximal humerus malunion with greater tuberosity healed lateral to the humeral diaphysis. *PHFS*, proximal humeral fracture sequelae; *3D*, three-dimensional; *CT*, computed tomography.

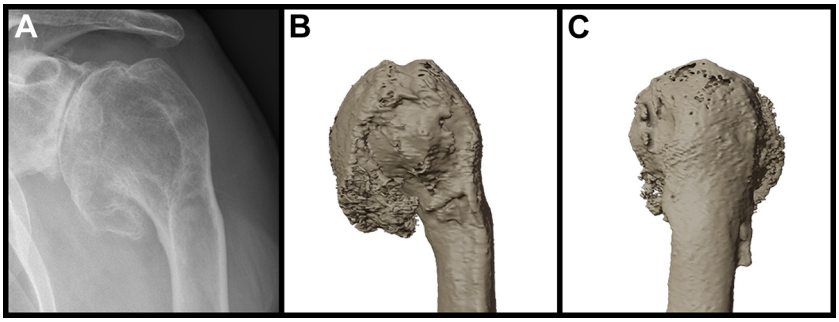

Figure 3 Type 1D PHFS. (**A**) true anteroposterior radiograph view, (**B**) coronal 3D CT scan, and (**C**) sagittal 3D CT scan view of a varus displaced proximal humerus malunion with greater tuberosity healed medial to the lateral cortex of the humeral diaphysis. *PHFS*, proximal humeral fracture sequelae; *3D*, three-dimensional; *CT*, computed tomography.

medial translation of the diaphysis and lateral cortex bone loss. In this setting, the use of a prosthetic stem, without correction of the deformity, would lead to an increased offset with excessive rotator cuff tension and joint stiffness (Fig. 2*A-C*).

- Type 1D – Varus displaced malunion with the greater tuberosity placed medial to the diaphysis; usually associated to humeral head retroversion, parasagittal posterior tilt, and medial and posterior calcar bone loss. The use of a prosthetic stem, without correction of the deformity, could increase the risk of fracture of the greater tuberosity and to create a prominence of the inferior part of the humeral head (Fig. 3*A-C*).
- Type 4A – Medial displacement of the greater tuberosity, associated to a reparable posterior rotator cuff; the humeral head could be aligned in varus, valgus, or non united (Fig. 4*A-C*).
- Type 4B –Medial dislocation of the greater tuberosity associated to a complete lack of posterior rotator cuff (Fig. 5*A-C*); the humeral head could be aligned in varus, valgus, or non united.

Planning of the MCHO

The 4 principles followed during the planning of MCHO were 1) the realignment of the humeral metaphysis and the shaft (in order to reduce the risk of intraoperative fracture during broaching), 2) a positioning of the fragments which might maximize the surface contact area between them, 3) the protection of the posterior rotator cuff tendons along with a minimum removal of bone, and 4) the preservation of the length of the humerus. Different patterns of surgery could be defined as follows:

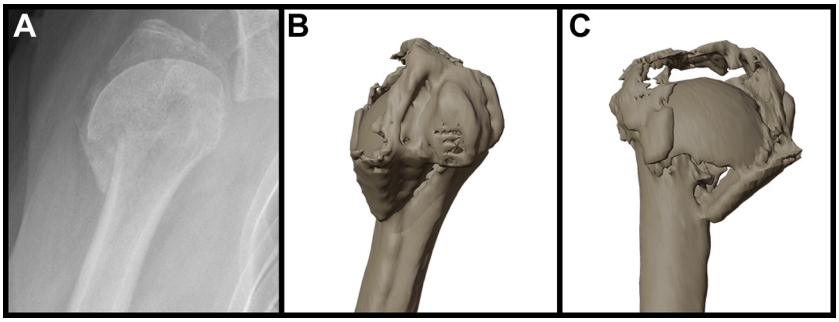

Figure 4 Type 4A PHFS. (**A**) true anteroposterior radiograph view, (**B**) coronal 3D CT scan, and (**C**) sagittal 3D CT scan view of a valgus displaced malunion with medial dislocation of the greater tuberosity respect the humeral head, and a reparable posterior rotator cuff. *PHFS*, proximal humeral fracture sequelae; *3D*, three-dimensional; *CT*, computed tomography.

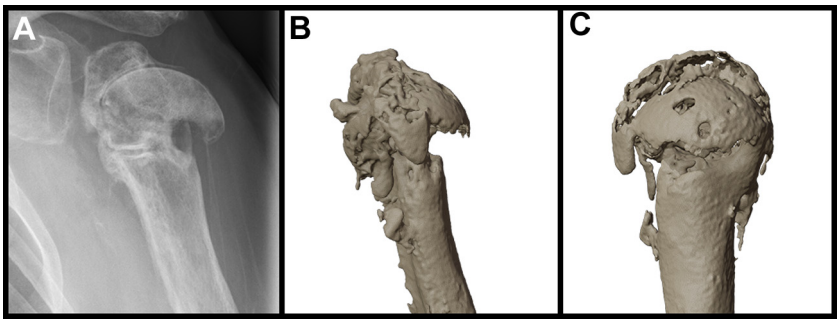

Figure 5 Type 4B PHFS. (**A**) true antero-posterior radiograph view, (**B**) coronal 3D CT scan, and (**C**) sagittal 3D CT scan view of a a valgus displaced malunion with medial dislocation of the greater tuberosity respect the humeral head, and an irreparable posterior rotator cuff. PHFS, proximal humeral fracture sequelae; 3D, three-dimensional; CT, computed tomography.

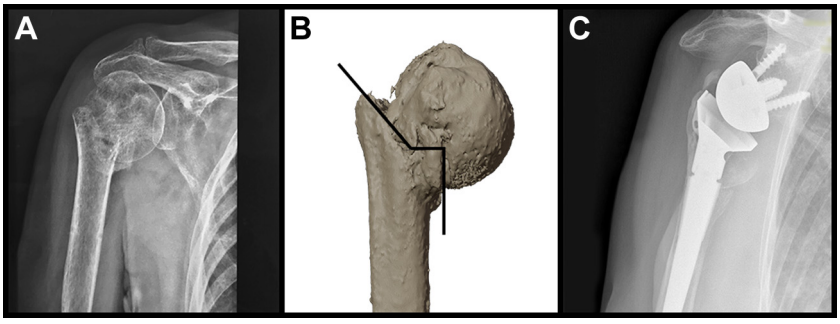

Figure 6 Reverse arthroplasty for type 1D PHFS. Preoperative (**A**) and postoperative (**B**) anteroposterior radiographs of a patient after linear osteotomy and reverse shoulder prosthesis implantation with medial calcar graft to compensate the medial bone loss. Number 2, non-resorbable, transosseous wires were used to fix the metaphysis and the calcar graft to the humeral stem and the diaphysis. *PHFS*, proximal humeral fracture sequelae.

- Anatomic or reverse arthroplasty for type 1C-1D

In the setting of TSA or rTSA, a linear metaphyseal osteotomy of the humerus was performed, as already published.[30] The metaphyseal osteotomy was first simulated in the coronal plane based on the differences between the affected and the healthy side. The same cut was then modified in the sagittal plane (in order to modulate the anteroposterior translation of the proximal humerus) and in the axial plane (in order to address the rotational component of the deformity). Intraoperatively, K-wires were placed into the cutting guides and were used as reference to assess the correct rotation. In order to avoid an excessive humeral shortening, a cuneiform resection was not considered. Once the osteotomy had been completed, the humeral prosthetic stem was handled as a nail ("shish-kebab" technique[6]). The metaphyseal fragment was fixed to the prosthetic stem and to the humeral diaphysis using non-resorbable, number 2, transosseous sutures. If needed, a humeral head bone graft could be used to fill the humeral bone loss secondary to the correction of the proximal humeral deformity (Fig. 6).

- Reverse arthroplasty for type 4A

If the greater tuberosity was healed but medially displaced, a patient-specific surgical guide was used to preserve it as a bony fragment during the osteotomy. This fragment was released from the surrounding adhesions and fixed through multiple non-resorbable, number 2, transosseous sutures to the prosthetic stem

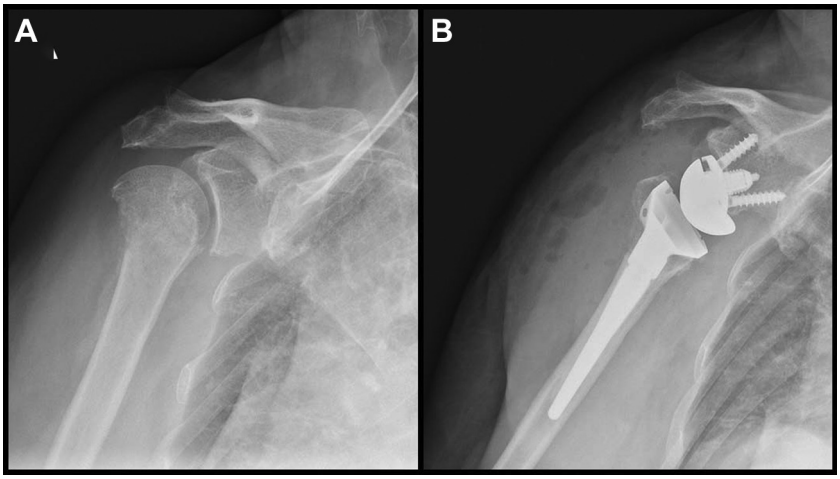

Figure 7 Reverse arthroplasty for type 4A PHFS. Preoperative (**A**) and postoperative (**B**) anteroposterior radiographs of a patient after greater tuberosity osteotomy and implantation of a reverse prosthesis. *PHFS*, proximal humeral fracture sequelae.

Figure 8 Anatomical patient-specific osteotomy guide used for a greater tuberosity osteotomy with a deltopectoral approach. Reproduced by permission of Russo R, Cozzolino A, Guastafierro A, Della Rotonda G, Viglione S, Ciccarelli M, Mortellaro M, Minopoli P, Fiorentino F, Pietroluongo LR, and Wolters Kluwer Health, Inc. Use of 3D planning and patient-specific guide for proximal humerus corrective osteotomy associated with shoulder prosthesis implantation in proximal humerus varus maluninon. Tech Hand Up Extrem Surg 2021. Further reproduction, distribution, or transmission is prohibited, except as otherwise permitted by law.

and to the humeral diaphysis. Indeed, the humeral stem could be inserted by resecting only a thin cartilagineous layer, keeping the dislocated humeral head in situ. A second surgical neck osteotomy was usually not required. (Fig. 7).

- Reverse arthroplasty for type 4B

In case of severe fatty infiltration of the rotator cuff muscles, or whenever the greater tuberosity could not be clearly identified, we performed a proximal humerus resection and we used a proximal humerus allograft to restore the humeral length, as previously published.[33] The posterior cuff on the allograft was sutured to the residual posterior scar tissue, with the aim to obtain a tenodesis effect and restore some external rotation. A 3D preoperative planning was used to perform correctly both the humeral and the allograft bone cuts, without any PSI.

Table III
Surgical procedure performed according to the type of PHFS.

	Type 1C	Type 1D	Type 4A	Type 4B	Total
No. of patientss	4	8	6	2	20
PSI	4	8	5	0	17
Isolated linear osteotomy SN	4	8	0	2	14
Isolated linear osteotomy GT	0	0	5	0	5
Multiple osteotomy (SN + GT)	0	0	1	0	1
Uncemented/cemented stem	2/2	8/0	4/2	0/2	14/6
BIO-RSA	1	0	2	1	4
Massive allograft	0	0	0	2	2

PHFS, proximal humeral fracture sequelae; *PSI*, patient-specific instrumentation; *SN*, surgical neck; *GT*, greater tuberosity; *BIO-RSA, bony*, increased offset reverse shoulder arthroplasty.

Design of PSI

Cutting guides were created to adapt uniquely to the specific anatomy of the patient, with 3 divergent K-wire holes to ensure adequate stability during the bone cut (Fig. 8). Guides were 3D printed using a biocompatible photopolymer resin. Before surgery, a simulation of the planned osteotomy was performed to verify the feasibility of the procedure and to anticipate potential critical points. On the day of the surgery, cutting guides were prepared in a hydrogen peroxide gas plasma sterilizer (STERRAD, Irvine, CA, USA), reducing the risk of volumetric or morphological changes.[36]

Collection of data

Preoperative data including age, sex, type and level of activity, date of the initial trauma, previous treatments, active range of movement, Constant Score (CS), visual analog scale (VAS), and Disabilities of the Arm, Shoulder and Hand (DASH) score, the positivity to the hornblower sign and the presence of the lag sign in external rotation were collected at baseline. Preoperative radiographs and CT scan (as already described) were recorded. Clinical scores and examinations (active range of movement, Hornblower sign, and lag sign) were further recorded at 1 and 2 y of follow-up. True anteroposterior, outlet and axillary shoulder radiographs were analyzed after surgery, at 1 and 2 y of follow-up. Scapular notching was graded according to the Sirveaux classification.[39] Greater tuberosity resorption was defined as partial or complete based on the comparison with radiographs taken immediately after surgery.

Table IV
Preoperative and 2-y follow-up clinical results according to the type of PHFS.

	N° of patients	CS mean ± SD		DASH mean ± SD		VAS mean ± SD		AAE mean ± SD (°)		AER mean ± SD (°)	
		Preop	24 M	Preop	24 M	Preop	24 M	Preop	24 M	Preop	24M
Type 1C	4	27 ± 7.7	69 ± 9.4	61.9 ± 4.9	18.3 ± 6.2	6.2 ± 1.1	1 ± 0.8	76 ± 26	135 ± 19	−7± 15	8 ± 7
Type 1D	8	25.6 ± 10.1	65.1 ± 12.8	59.2 ± 11	32 ± 18.8	7 ± 1.7	1.5 ± 1.2	79 ± 20	131 ± 20	−10 ± 17	12 ± 10
Type 4A	6	23.2 ± 7.4	74.6 ± 3.3	60.3 ± 10.8	18.4 ± 6.8	6.2 ± 0.9	1.8 ± 0.8	62 ± 12	160 ± 8	−14 ± 10	25 ± 15
Type 4B	2	17 ± 2	60 ± 15	65.2 ± 2.3	29.6 ± 5.6	6.5 ± 0.5	2.5 ± 0.5	55 ± 5	130 ± 30	−20 ± 10	5 ± 5
Total	20	24.3 ± 8.8	67.7 ± 11.4	60.7 ± 9.6	24.1 ± 13.1	6.5 ± 1.3	1.6 ± 0.8	72 ± 18	139 ± 21	−12 ± 13	13 ± 12

SD, standard deviation; *CS*, Constant Score; *DASH*, Disabilities of the Arm, Shoulder and Hand; *VAS*, visual analog scale; *AAE*, active anterior elevation; *AER*, active external rotation at side; *PHFS*, proximal humeral fracture sequelae.

Table V
Clinical parameter scores for all the patients at T0 (preoperative), T1 (12 mo), and T2 (24 mo). Multi-comparison tests were performed with ANOVA test for repeated measures into groups and the Bonferroni correction (B) of *P*-value was used in pairwise comparison into groups between two consecutive control points. Scores are indicated as mean ± standard deviation.

	T0	T1	T2	*P*-value
CS	24.3 ± 8.8	67.2 ± 8.7	67.7 ± 11.4	< .001 (ANOVA) T0-T1 = <.001 (B) T1-T2 = 1 (B)
DASH	60.7 ± 9.6	24 ± 6.9	24.1 ± 13.1	< .001 (ANOVA) T0-T1 = <.001 (B) T1-T2 = 1 (B)
VAS	6.5 ± 1.3	1.5 ± 0.7	1.6 ± 0.8	< .001 (ANOVA) T0-T1 = <.001 (B) T1-T2 = 1 (B)
AAE (°)	70 ± 21,4	142 ± 29,3	140 ± 25,5	< .001 (ANOVA) T0-T1 = <.001 (B) T1-T2 = 1 (B)
AER (°)	−9,4 ± 16,2	13,3 ± 11,5	15,4 ± 12,9	< .001 (ANOVA) T0-T1 = <.001 (B) T1-T2 = 1 (B)

AAE, active anterior elevation; *AER*, active external rotation at side; *CS*, Constant Score; *DASH*, Disability of the Arm, Shoulder and Hand questionnaire; *VAS*, visual analog scale; *ANOVA*, analysis of variance.

Glenoid or humeral loosening was defined as migration or rotation of the respective component. Humeral stem radiolucencies were classified according to Sanchez-Sotelo et al.[32,34] Humeral stress shielding was evaluated according to Nagels et al.[20]

Statistical analysis

Data were reported as mean ± standard deviation or as numbers (percentages). The values were tested for normal distribution using the Shapiro-Wilk test. Comparison between preoperative clinical scores (CS, DASH, VAS, active anterior elevation, active external rotation at side) and 1- and 2-y follow-up values was performed using an ANOVA with Bonferroni correction. Univariate analysis was carried out to test demographics (sex and age), clinical variables (interval between the initial trauma and the definitive surgery, type of previous treatment [conservative vs surgical], type of PHFS), radiological variables (10 CT-based variables which have been described above), and surgical variables (type of surgery) against all clinical scores at baseline (T0), 1-y (T1), and 2-y (T2) follow-up, using Pearson's correlation (for continuous variables) or point-biserial correlation (for categorical variables). The degree of correlation was judged as high for coefficient values between 0.5 and 1, moderate between 0.3 and 0.49, and low if lower than 0.29. Variables showing a statistically significant association were included in a multivariate model in order to identify predictors of outcome. The level of significance was set at $P < .05$. Statistical analysis was performed using Statistical Package for Social Sciences (SPSS) Version 20.0 (IBM, Armonk, NY, USA).

Results

Study population

Twenty-nine patients were initially included in the study. Six patients were excluded due to an infection detected during the first of a 2-stage procedure. Two patients treated with an isolated MCHO fixed with plate and screws were also excluded. One patient died after coronavirus (COVID-19) infection before completing the 2-y follow-up, leaving 20 patients available for the final analysis. All patients were operated by the senior author (R.R.). Thirteen patients had initially been treated conservatively while 7 patients had undergone surgery (percutaneous pinning and locking plate in 3 and 4 cases, respectively). The mean time between the initial trauma and the inclusion in the study was 25.2 mo (range 3 to 156).

In 6 patients, we could not use the contralateral side CT scan to complete the preoperative 3D evaluation of the deformity. Indeed, 4 patients were affected by a previous controlateral humerus fracture, 1 patient was previously operated with rTSA, and in 1 patient we decided to not repeat the CT scan after motion artifact.

According to the above discussed classification, we defined 4 cases as type 1C, 8 as 1D, 6 as 4A, and 2 as 4B. Preoperative clinical and radiological parameters, according to the specific subgroup of inclusion, have been depicted in Table II.

Surgical procedure

Surgical procedure details according to the type of PHFS are presented in Table III.

In all patients, an inlay 155° stem and a 36° glenosphere (SMR LIMA, Italy) were used. In 14 patients, (70%) a cementless stem was implanted. In 2 patients, affected by type 4B PHFS, a proximal humerus allograft with the attached posterior rotator cuff tendon was used.

A linear humeral neck osteotomy was performed in 14 cases, an isolated greater tuberosity osteotomy in 5 cases, and multiple osteotomies (both humeral neck and greater tuberosity) in 1 case. In 2 cases, a 2-stage surgery was needed (metalwork removal followed by a definitive procedure). In 17 cases, PSI was 3D printed and in 2 cases the preoperative planning was modified during surgery. Specifically, in one patient initially classified as 4A and scheduled to have a double osteotomy (greater tuberosity and surgical neck) the greater tuberosity was intraoperatively deemed to be in an acceptable position and a decision to perform only the surgical neck osteotomy was made. This patient was then reclassified as type 1D. In another patient, initially classified as 4B and for which an allograft of the proximal humerus had been prepared, teres minor was found intact (type 4A). As such, the allograft was not used.

Clinical outcome

The mean (± standard deviation) CS, VAS, and DASH values improve from 24.3 (± 8.8), 6.5 (± 1.3), 60.7 (± 9.6) preoperatively, to

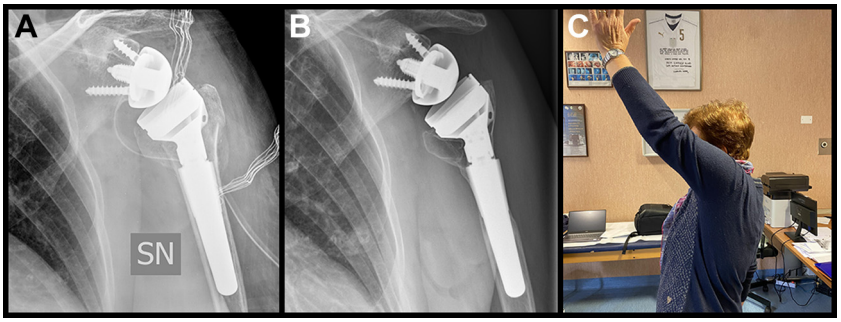

Figure 9 Postoperative greater tuberosity resorption and humeral lateral cortex stress shielding, 2 years after RSA associated with MCHO. Postoperative (**A**) and 2 year follow-up (**B**) anteroposterior radiograph showing partial tuberosity resorption not associated to loss of forward elevation and external rotation (**C**). Written informed consent was obtained from the patient(s) for their anonymized information and for clinical pictures to be published in this article. *RSA*, reverse shoulder arthroplasty; *MCHO*, multiplanar corrective humeral osteotomy.

67.7 (± 11.4), 1.6 (± 0.8), 24.1 (± 13.1) points after surgery, respectively (Tables IV and V). A statistically significant improvement was observed already at 1 y of follow-up (Table V). The minimally clinical important difference for CS and DASH score [41] was achieved in 95% of patients. The clinical outcome remained stable at 1- and 2-y follow-up except for one patient, aged 78, affected by a type 1D PHFS, in which the CS decreased between the 1- and 2-y follow-up (from 60 to 38 points) with no radiological evidence of resorption of the greater tuberosity.

In the 2 patients for which a massive allograft was necessary, even if the hornblower sign remained positive, we documented a mean gain of active external rotation (from -30° and 10°) and active external rotation in adduction (from -10° to 0°) by 30°, with a DASH score of 24 and 35.3 points.

Complications

No intraoperative complication was recorded. An overall postoperative complication rate of 10% was observed. One patient presented with a postoperative wound drainage, successfully treated with antibiotics and vacuum therapy. Scapular notching grade 1 and grade 2 were observed in 4 (20%) and 1 cases (5%), respectively. In 1 case affected by type 1D PHFS, a partial resorption of the greater tuberosity associated to lateral cortex stress shielding graded as L2 was observed at the radiological 2-y follow-up, with no clinical impact on the patient (Fig. 9).

Predictors of outcome

At the univariate analysis, age correlated moderately but significantly with the CS (negative correlation; R = -0.4; $P = .004$) and VAS (positive correlation, R = 0.39; $P = .048$) at baseline. No significative difference was observed between patients affected by type 1 and 4 PHFS. No other correlation was found between all the included variables and the clinical score.

Discussion

The most important finding of this study is that MCHO in combination with rTSA is a viable option to treat PHFS. In this series, the adoption of the preoperative 3D planning and PSI allowed to obtain a significant clinical improvement at 1 y of follow-up, which was maintained until 2 y from surgery. The overall complication rate of 10% was deemed encouraging, especially considering the complexity of the procedures described. Furthermore, although we were unable to identify clear predictors of outcome, we reported a precise algorithm of treatment to tackle a heterogeneous, insidious, and challenging condition as PHFS.

Looking upon the literature, it has been showed that the current tendency to treat proximal humeral fractures in a conservative way might increase the risk of symptomatic malunion and PHFS.[14] In this latter case, should the patient undergo rTSA, an accurate placement of the stem could be technically difficult with a high rate of complications.[6,8,18,22] In order to correct humeral deformities without performing an osteotomy of the greater tuberosity, Neer recommended to ream eccentrically the medullary canal and to use an undersized humeral stem placed in a nonanatomic position.[21] Conversely, other authors have proposed to use stemless or onlay stem prostheses.[3,15,28] Of note, Ballas et al reported the results of 27 patients which had received an anatomic stemless implant for type 1 (19 cases), type 2 (2 cases), and type 4 (6 cases) PHFS, without osteotomy of the greater tuberosity. At a mean follow-up of 44 mo, a similar CS for the different PHFS types (approximately 61 points) was found, with one case of revision (4%) to rTSA at 1 y due to rotator cuff failure.[3] In our experience, stemless implants do not represent a solution for all situations. As an example, in case of previous osteosynthesis, the poor bone quality of the proximal humerus might jeopardize the primary stability of a prosthesis. Also, it should be considered that a nonanatomic positioning of a stemless prosthesis could reduce the survivorship of the implant.

Total shoulder arthroplasty (either anatomic or reverse) for type 1C, 1D, 3, and 4 PHFS is associated with a high rate of postoperative complications. Previous studies reported an intraoperative fracture rate between 6.8% and 33%.[6,19,25,26] In a review including 9 studies and 234 patients affected by PHFS (without any distinction about subtype) treated with rTSA, Holton et al reported a 29% rate of severe complication (dislocation in 16.7%, infection in 6.8%, periprosthetic fracture in 3%, and nerve injury in 2.6% of cases) .[14] In 2020, Boileau et al reported the results achieved in 98 patients presenting with PHFS, undergone rTSA and followed at a minimum of 5 y. Out of them, in 40 patients (affected by type 3 and 4 PHFS) the authors additionally performed a greater tuberosity osteotomy or excision, which was associated to a poorer clinical outcome (CS of 59 vs 49 points), a higher complication rate (6% vs 33%), and a shorter survival rate of the implant (100% vs 85%) .[6] Conversely, in our series rTSA in combination with MCHO enabled a more satisfactory clinical outcome at 2 y (CS 67 points) along with a lower complication rate (10%). Nevertheless, we observed a limitation of active external rotation (mean 13°), in contrast to the value observed in patients operated with rTSA for other etiologies.[45] It should be emphasized that Boileau et al did not distinguish the results found after greater tuberosity osteotomy or excision, neither reported details about the timeframe in which the bone resorption

of the tuberosity occurred. In our opinion, at least 4 elements should be considered in order to potentially explain our results. First, in our series, only 35% of PHFSs (as compared to 53% in the study by Boileau et al) had previously undergone a surgical treatment, which in turn may negatively affect the bone quality of the proximal humerus. Second, we used a cementless stem in 70% of cases (as compared to 6% of cases reported in the Boileau's series). Taking into account a hypothetical negative impact of cement on the healing process, these stems potentially contributed to obtain a positive result in our cohort.[38] Third, the use of reverse allograft prosthesis composite, in case of proximal humerus resection for PHFS type 4B, could improve clinical outcome in the cases in which Boileau reported the worst results. Lastly, the preoperative 3D planning associated with PSI used in the majority of patients might have helped perform a more accurate bone cut and achieve a more precise final positioning of the bony fragments.

The authors acknowledge some limitations in this study. Primarily, the lack of a control group. Although the presence of a comparative group treated 'without MCHO' would have been helpful, we think that the algorithm reported in this study might represent a keystone for future comparative analyses. Second, the small number of patients should be taken into account. However, this was partially due both to the strict inclusion criteria and to the relative short time interval of the study. Third, no subgroup analysis regarding different types of PHFS was carried out in this study. Fourth, the relatively short follow-up. However, the documentation of clinical results at 1 and 2 y seem to suggest a relative stability of results over time, which of course will need confirmation or disproving in further studies.

Conclusion

The combination of preoperative 3D planning and intraoperative use of 3D-printed PSI to perform MCHO as concurrent procedure in the context of rTSA in the treatment of Boileau type 1C, 1D, and 4 PHFS may lead to a satisfactory clinical outcome which is maintained at 2 y of follow-up. Further studies are warranted in order to shed some further light on the value of MCHO in each type of PHFS and to validate the algorithm proposed in this series.

Acknowledgments

The authors would like to acknowledge Andrea Vitale PhD, Research and Development Department, Pineta Grande Hospital.

Disclaimers:

Funding: No funding was disclosed by the authors.
Conflicts of interest: Dr Livia Renata Pietroluongo and Raffaele Russo are cofounders in an innovative start-up: E-lisa Srl. The Company is focused on R&D, consultancy and formation in Orthopedic & Trauma fields. These authors wish to confirm that there are conflicts of interest associated with this publication. The other authors, their immediate families, and any research foundation with which they are affiliated have not received any financial payments or other benefits from any commercial entity related to the subject of this article.
Patient consent: Written informed consent was obtained from the patient(s) for their anonymized information and for clinical pictures to be published in this article.

References

1. Abdelhady AM. Shoulder arthroplasty as a treatment for sequelae of proximal humeral fractures. Eur J Orthop Surg Traumatol 2010;20:607-11. https://doi.org/10.1007/s00590-010-0630-8.
2. Antuña SA, Sperling JW, Sánchez-Sotelo J, Cofield RH. Shoulder arthroplasty for proximal humeral malunions: long-term results. J Shoulder Elbow Surg 2002;11:122-9. https://doi.org/10.1067/mse.2002.120913.
3. Ballas R, Teissier P, Teissier J. Stemless shoulder prosthesis for treatment of proximal humeral malunion does not require tuberosity osteotomy. Int Orthop 2016;40:1473-9. https://doi.org/10.1007/s00264-016-3138-y.
4. Beredjiklian PK, Iannotti JP, Norris TR, Williams GR. Operative treatment of malunion of a fracture of the proximal aspect of the humerus. J Bone Joint Surg Am 1998;80:1484-97.
5. Boileau P, Chuinard C, Le Huec JC, Walch G, Trojani C. Proximal Humerus Fracture Sequelae:impact of a new radiographic classification on arthroplasty. Clin Orthop Relat Res 2006;442:121-30. https://doi.org/10.1097/01.blo.0000195679.87258.6e.
6. Boileau P, Seeto BL, Clowez G, Gauci MO, Trojani C, Walch G, et al. SECEC Grammont Award 2017: the prejudicial effect of greater tuberosity osteotomy or excision in reverse shoulder arthroplasty for fracture sequelae. J Shoulder Elbow Surg 2020;29:2446-58. https://doi.org/10.1016/j.jse.2020.03.010.
7. Boileau P, Trojani C, Walch G, Krishnan SG, Romeo A, Sinnerton R. Shoulder arthroplasty for the treatment of the sequelae of fractures of the proximal humerus. J Shoulder Elbow Surg 2001;10:299-308.
8. Boileau P, Watkinson D, Hatzidakis AM, Hovorka I. Neer Award 2005: the Grammont reverse shoulder prosthesis. Results in cuff tear arthritis, fracture sequelae, and revision arthroplasty. J Shoulder Elbow Surg 2006;15:527-40. https://doi.org/10.1016/j.jse.2006.01.003.
9. Boileau P, Walch G. The three-dimensional geometry of the proximal humerus. Implications for surgical technique and prosthetic design. J Bone Joint Surg Br 1997;79:857-65.
10. Cicak N, Klobucar H, Medancic N. Reverse shoulder arthroplasty in acute fractures provides better results than in revision procedures for fracture sequelae. Int Orthop 2015;39:343-8. https://doi.org/10.1007/s00264-014-2649-7.
11. Duparc F. Malunion of the proximal humerus. Orthop Traumatol Surg Res 2013;99:S1-11. https://doi.org/10.1016/j.otsr.2012.11.006.
12. Fürnstahl P, Schweizer A, Graf M, Vlachopoulos L, Fucentese S, Wirth S, et al. Surgical treatment of long-bone deformities: 3d preoperative planning and patient-specific instrumentation. Lect Notes Comput Vis Biomech 2016;23:123-49. https://doi.org/10.1007/978-3-319-23482-3_7.
13. Greiner S, Uschok S, Herrmann S, Gwinner C, Perka C, Scheibel M. The metaphyseal bone defect predicts outcome in reverse shoulder arthroplasty for proximal humerus fracture sequelae. Arch Orthop Trauma Surg 2014;134:755-64. https://doi.org/10.1007/s00402-014-1980-1.
14. Holton J, Yousri T, Arealis G, Levy O. The role of reverse shoulder arthroplasty in management of proximal humerus fractures with fracture sequelae: a systematic review of the literature. Orthop Rev (Pavia) 2017;24:6977. https://doi.org/10.4081/or.2017.6977.
15. Huguet D, DeClercq G, Rio B, Teissier J, Zipoli B, TESS Group. Results of a new stemless shoulder prosthesis: radiologic proof of maintained fixation and stability after a minimum of three years' follow-up. J Shoulder Elbow Surg 2010;19:847-52. https://doi.org/10.1016/j.jse.2009.12.009.
16. Kamer L, Noser H, Popp AW, Lenz M, Blauth M. Computational anatomy of the proximal humerus: an *ex vivo* high-resolution peripheral quantitative computed tomography study. J Orthop Translat 2015;4:46-56. https://doi.org/10.1016/j.jot.2015.09.006.
17. Mansat P, Bonnevialle N. Treatment of fracture sequelae of the proximal humerus: anatomical vs reverse shoulder prosthesis. Int Orthop 2015;39:349-54. https://doi.org/10.1007/s00264-014-2651-0.
18. Mansat P, Guity MR, Bellumore Y, Mansat M. Shoulder arthroplasty for late sequelae of proximal humeral fractures. J Shoulder Elbow Surg 2004;13:305-12. https://doi.org/10.1016/j.jse.2004.01.020.
19. Moineau G, McClelland WB, Trojani C, Rumian A, Walch G, Boileau P. Prognostic factors and limitations of anatomic shoulder arthroplasty for the treatment of posttraumatic cephalic collapse or necrosis (type-1 proximal humeral fracture sequelae). J Bone Joint Surg Am 2012;94:2186-94. https://doi.org/10.2106/JBJS.J.00412.
20. Nagels J, Stokdijk M, Rozing PM. Stress shielding and bone resorption in shoulder arthroplasty. J Shoulder Elbow Surg 2003;12:35-9. https://doi.org/10.1067/mse.2003.22.
21. Neer CS. Old trauma in glenohumeral arthroplasty. Shoulder reconstruction, 222-34. Philadelphia: Saunders; 1990, ISBN 978-0721628325.
22. Norris TR, Green A, McGuigan FX. Late prosthetic shoulder arthroplasty for displaced proximal humerus fractures. J Shoulder Elbow Surg 1995;4:271-80.
23. Pastor MF, Kieckbusch M, Kaufmann M, Ettinger M, Wellmann M, Smith T. Reverse shoulder arthroplasty for fracture sequelae: clinical outcome and prognostic factors. J Orthop Sci 2019;24:237-42. https://doi.org/10.1016/j.jos.2018.09.016.
24. Pinkas D, Wanich TS, Depalma AA, Gruson KI. Management of malunion of the proximal humerus: current concepts. J Am Acad Orthop Surg 2014;22:491-502. https://doi.org/10.5435/JAAOS-22-08-491.
25. Raiss P, Alami G, Bruckner T, Magosch P, Habermeyer P, Boileau P, et al. Reverse shoulder arthroplasty for type 1 sequelae of a fracture of the proximal humerus. Bone Joint J 2018;100-B:318-23. https://doi.org/10.1302/0301-620X.100B3.BJJ-2017-0947.R1.
26. Raiss P, Bradley Edwards T, Collin P, Bruckner T, Zeifang F, Loew M, et al. Reverse shoulder arthroplasty for malunions of the proximal part of the

humerus (type-4 fracture sequelae). J Bone Jt Surg Am 2016;98:893-9. https://doi.org/10.2106/JBJS.15.00506.
27. Ranalletta M, Bertona A, Rios JM, Rossi LA, Tanoira I, Maignon GD, et al. Corrective osteotomy for malunion of proximal humerus using a custom-made surgical guide based on three-dimensional computer planning: case report. J Shoulder Elbow Surg 2017;26:e357-63. https://doi.org/10.1016/j.jse.2017.08.002.
28. Romano AM, Braile A, Casillo P, Nastrucci G, Susanna M, Di Giunta A, et al. Onlay uncemented lateralized reverse shoulder arthroplasty for fracture sequelae type 1 with valgus/varus malunion: deltoid lengthening and outcomes. J Clin Med 2020;9:3190. https://doi.org/10.3390/jcm9103190.
29. Rosseels W, Herteleer M, Sermon A, Nijs S, Hoekstra H. Corrective osteotomies using patient-specific 3D-printed guides: a critical appraisal. Eur J Trauma Emerg Surg 2019;45:299-307. https://doi.org/10.1007/s00068-018-0903-1.
30. Russo R, Cozzolino A, Guastafierro A, Della Rotonda G, Viglione S, Ciccarelli M, et al. Use of 3D planning and patient-specific guides for proximal humerus corrective osteotomy associated with shoulder prosthesis implantation in proximal humeral varus malunion. Tech Hand Up Extrem Surg 2021;10:131-8. https://doi.org/10.1097/BTH.0000000000000372.
31. Russo R, Visconti V, Ciccarelli M, Cautiero F, Gallo M. Malunion of complex proximal humerus fractures treated by biplane and triplane osteotomy. Tech Shoulder Elb Surg 2008;9:70-5. https://doi.org/10.1097/BTE.0b013e318169e968.
32. Sanchez-Sotelo J, O'Driscoll SW, Torchia ME, Cofield RH, Rowland CM. Radiographic assessment of cemented humeral components in shoulder arthroplasty. J Shoulder Elbow Surg 2001;10:526-31.
33. Sanchez-Sotelo J, Wagner ER, Sim FH, Houdek MT. Allograft-prosthetic composite Reconstruction for massive proximal humeral bone loss in reverse shoulder arthroplasty. J Bone Joint Surg Am 2017;99:2069-76. https://doi.org/10.2106/JBJS.16.01495.
34. Sanchez-Sotelo J, Wright TW, O'Driscoll SW, Cofield RH, Rowland CM. Radiographic assessment of uncemented humeral components in total shoulder arthroplasty. J Arthroplasty 2001;16:180-7.
35. Santana F, Alentorn-Geli E, Guirro P, Torrens C. Reverse shoulder arthroplasty for fracture sequelae: how the initial fracture treatment influences the outcomes of joint replacement. Acta Orthop Traumatol Turc 2019;53:278-81. https://doi.org/10.1016/j.aott.2019.03.010.
36. Shaheen E, Alhelwani A, Van De Casteele E, Politis C, Jacobs R. Evaluation of dimensional changes of 3D printed models after sterilization: a pilot study. Open Dent J 2018;31:72-9. https://doi.org/10.2174/1874210601812010072.
37. Siegel JA, Dines DM. Techniques in managing proximal humeral malunions. J Shoulder Elbow Surg 2003;12:69-78. https://doi.org/10.1067/mse.2002.123902.
38. Singh A, Padilla M, Nyberg EM, Chocas M, Anakwenze O, Mirzayan R, et al. Cement technique correlates with tuberosity healing in hemiarthroplasty for proximal humeral fracture. J Shoulder Elbow Surg 2017;26:437-42. https://doi.org/10.1016/j.jse.2016.08.003.
39. Sirveaux F, Favard L, Oudet D, Huquet D, Walch G, Mole D. Grammont inverted total shoulder arthroplasty in the treatment of glenohumeral osteoarthritis with massive rupture of the cuff: results of a multicentre study of 80 shoulders. J Bone Joint Surg Br 2004;86:388-95. https://doi.org/10.1302/0301-620x.86b3.14024.
40. Solonen KA, Vastamäki M. Osteotomy of the neck of the humerus for traumatic varus deformity. Acta Orthop 1985;56:79-80.
41. Su F, Allahabadi S, Bongbong DN, Feeley BT, Lansdown DA. Minimal clinically important difference, substantial clinical benefit, and patient acceptable symptom state of outcome measures relating to shoulder pathology and surgery: a systematic review. Curr Rev Musculoskelet Med 2021;14:27-46. https://doi.org/10.1007/s12178-020-09684-2.
42. Takahashi K, Morita Y, Ohshima S, Izumi S, Kubota Y, Yamamoto Y, et al. Creating an optimal 3D printed model for temporal bone dissection training. Ann Otol Rhinol Laryngol 2017;126:530-6. https://doi.org/10.1177/0003489417705395.
43. Vlachopoulos L, Schweizer A, Meyer DC, Gerber C, Fürnstahl P. Three-dimensional corrective osteotomies of complex malunited humeral fractures using patient-specific guides. J Shoulder Elbow Surg 2016;25:2040-7. https://doi.org/10.1016/j.jse.2016.04.038.
44. Vlachopoulos L, Schweizer A, Meyer DC, Gerber C, Fürnstahl P. Computer-assisted planning and patient-specific guides for the treatment of midshaft clavicle malunions. J Shoulder Elbow Surg 2017;26:1367-73. https://doi.org/10.1016/j.jse.2017.02.011.
45. Wellmann M, Struck M, Pastor MF, Gettmann A, Windhagen H, Smith T. Short and midterm results of reverse shoulder arthroplasty according to the preoperative etiology. Arch Orthop Trauma Surg 2013;133:463-71. https://doi.org/10.1007/s00402-013-1688-7.
46. Willis M, Min W, Brooks JP, Mulieri P, Walker M, Pupello D, et al. Proximal humeral malunion treated with reverse shoulder arthroplasty. J Shoulder Elbow Surg 2012;21:507-13. https://doi.org/10.1016/j.jse.2011.01.042.